Understanding the Effect of Ni Content on Microstructure and Mechanical Properties of A384 HPDC Alloy

Hüseyin Demirtaş[1], Erdem Karakulak[2], Nadendla Hari Babu[2]

[1]TOBB Technical Science Vocational School, Karabuk University, Turkey

[2]BCAST, Brunel University, Kingston Lane, Uxbridge, Middlesex, UB8 3PH, United Kingdom

Abstract

Investigations have been carried out to understand the correlation between Ni content and properties of HPDC cast A384 aluminium alloy in as-cast and heat-treated conditions. Depending on Ni content in the alloy, different Ni-bearing intermetallics were formed. Suitable heat treatment conditions were selected after a series of experiments to obtain optimal mechanical properties. Most of the Ni containing intermetallics found to be stable at solutionizing temperatures which have a dramatic effect on the mechanical properties of alloys after natural and artificial aging. The results showed that, after heat treatment, to achieve higher strength values lower Ni additions are favourable.

Keywords: Aluminium, HPDC, Intermetallic, Heat-treatment, Mechanical properties.

1. Introduction

Al-11Si-4Cu (A384) aluminium alloy parts cast by high pressure die casting (HPDC) process are widely used in automotive industry for applications like cylinder blocks/heads and fuel pumps [1]. The main reasons of selecting this alloy are its castability, high strength to weight ratio, machinability, and also the possibility of improving the properties with heat treatments. Other than silicon this alloy contains Cu in order to increase strength, Fe to achieve an easy release of the cast parts from the die, and Mn to overcome the detrimental effects of Fe [2–5]. The silicon level of the A384 alloy is very close to the eutectic point in the Al-Si binary phase diagram which means that the microstructure is consisting of Al-Si eutectic phase with a small amount of α-Al dendrites and different intermetallic phases. Although HPDC process provides high cooling rates some coarse and needle-shaped eutectic silicon crystals can exist in the microstructure of the material. It is known that needle-shaped silicon crystals are detrimental for the mechanical properties of the alloys especially for ductility, to avoid these effects needle-shaped silicon crystals need to be modified [6–8]. Previous studies showed that sodium (Na), strontium (Sr), and antimony (Sb) have modifying effect on the Si

crystals in Al-Si alloys. Among the three, Sr is by far the most efficient and effective modifier due to the handling difficulty of sodium and the toxicity of the antimony [9–12].

Nickel is usually added to A384 alloy to improve the properties of the material. There are numerous studies in the literature reporting results of Ni addition to Al alloys containing Si and Cu. The addition of Ni to Al alloys causes the formation of intermetallic compounds even at low concentrations because of the very limited solubility of Ni in solid Al [13–17]. Most of the existing studies about Ni addition to similar alloys reported that Ni collaborates with Cu and Fe to form new intermetallic phases or react with the existing intermetallics to change their chemical composition [9]. Possible reported intermetallics that might form with the addition of Ni are Al_3CuNi, Al_7Cu_4Ni, Al_9FeNi, $Al_3(Cu,Ni)_2$, Al_3Ni, Al_3Ni_2 [18–22]. Some of these phases are reported to be thermally stable at relatively high temperatures [16]. It is also reported that the addition of Ni favours the formation of Al_9FeNi phase instead of the brittle Al_5FeSi phase [5].

Because of the nature of the HPDC process, the gas content inside the cast parts can be as high as 12cc/100g [2]. This high gas content may cause formation of blisters on the surface of the cast parts during heat treatment. To prevent blistering the heat treatment temperature and duration should be selected as low as possible and as short as possible respectively [23]. The main aims of heat treatment are to change the morphology of silicon particles from flake-like to spheres and also to dissolve as much as solute atoms to precipitate during aging treatment to increase the strength of the material. Previous studies reported that 10 minutes of heat treatment at 540 ˚C is enough for complete spheroidization of silicon particles in an alloy with 7 % Si (All compositions are given in wt.-% hereafter, unless otherwise specified) [2]. Although prolonged heat treatment durations help to dissolve more solute atoms this may cause coarsening of silicon particles as well as blister formation.

In many standards for HPDC cast Al-Si-Cu based alloys (as 333, 360, 380, 384, etc.) the upper limit for Ni is set as 0.5 % [24]. On the other hand, most of the available literature about the effects of Ni on microstructure and mechanical properties of Al-Si-Cu alloys are related to additions of more than 1 % Ni [2, 9, 25]. Studies that have investigated the effect of smaller amounts of Ni are very limited [26, 27]. Effects of different nickel additions close to the widely accepted upper limit (e.g., 0.5 %) on mechanical properties remain unclear. An improved understanding of these effects in relation to the microstructural changes would facilitate opportunities for improving the properties of Al-Si-Cu based HPDC alloys.

In the present study sensitivity of the Ni content on the microstructure and mechanical properties of A384 alloy was investigated. The main aim is to understand the effects of different nickel additions

on formation of various phases in the as-cast and heat-treated conditions and to correlate these changes in the microstructure with the mechanical properties of the material.

2. Experimental

In this study, the commercial A384 HPDC alloy was used as the base alloy. Melting of the ingots realized in clay bonded graphite crucibles using an electrical resistance furnace. Al-10Ni and Al-10Sr master alloys were used for Ni and Sr additions. After all alloying additions, the melt was degassed using a rotary degasser with a graphite head. Degassing was conducted at 740 ˚C for 10 minutes with an argon flow rate of 4l/min and head rotation speed of 350 rpm. After degassing melt surface was skimmed using a boron nitride-coated steel tool and the melt temperature was dropped to the selected casting temperature of 710 ˚C. Casting was done using a 4500kN cold chamber HPDC machine. Eight ASTM B557 standard cylindrical samples with a gauge dimension of Ø6.35 mm x 50 mm were obtained in each casting, further information about the geometry of the cast part can be found elsewhere [28]. The cast samples were tested without any machining. The chemical compositions of the prepared alloys were analysed using an optical emission spectrometer (Oxford Instruments Foundry-Master Pro). Results of the chemical analysis of the cast samples are given in Table 1 with the standard composition of A384 alloy. As can be seen from the table Ni content of the alloys are below the limit, on the limit value, and above the limit of the standard composition of the A384 alloy.

Table1. Chemical composition of alloys

	Al	Si	Cu	Ni	Sr	Mg	Mn	Fe	Others
A384*	Bal.	10.5-12	3-4.5	Max 0.5	-	Max 0.1	Max 0.5	Max 1.3	
Sample 1	Bal.	11.50	3.82	0.28	0.02	0.30	0.21	0.75	<0.2
Sample 2	Bal.	11.10	3.74	0.52	0.02	0.29	0.21	0.74	<0.2
Sample 3	Bal.	10.50	3.61	0.91	0.02	0.28	0.20	0.75	<0.2

*Standard chemical composition of A384 alloy [24]

Heat treatments of the cast samples were conducted using an electrical resistance furnace. The furnace temperature was controlled using a K-type thermocouple and it was reported the change in the furnace temperature was less than ± 2 ˚C during the heat treatments. Quenching of samples after solutionizing heat treatments was realized by immersing the samples into room temperature water. Initial heat treatments were conducted on small samples cut from the cast tensile bars to determine the optimum heat treatment conditions, results of these initial experiments are explained in the

results section in detail. Hardness measurements were conducted using a Buehler Vickers microhardness tester with a load of 500 g and a dwelling time of 10 seconds. All reported hardness values are an average of 10 measurements. Instron 5500 Universal tester was used for the tensile tests. The gauge length of the extensometer used was 50 mm and the selected extension rate was 1 mm/min. Microstructures of as-cast and heat-treated samples were examined by Zeiss optical microscope (OM) and a Jeol JCM 6000Plus scanning electron microscope (SEM) equipped with energy-dispersive X-ray spectroscopy (EDS). The specimens for OM and SEM analysis were prepared by standard grinding and polishing procedures with a final polishing of 0.04 μm colloidal silica. SEM observations were performed after etching the samples with Keller's reagent (1% HF + 1.5% HCl + 2.5% HNO_3 + 95% H_2O).

3. Results and Discussion

3.1. Selection of Heat Treatment Conditions

Heat treatment of HPDC cast parts can be problematic because of the high hydrogen content of the material. This high hydrogen content caused by the nature of the HPDC process can end up with the formation of blisters on the surface of the material during heat treatment. Blister formation increases with increased heat treatment temperature and time. On the other hand, the main idea of the heat treatment which is applied to the Cu containing Al alloys is to dissolve as much as solute in α-Al in solution heat treatment step and then obtain the formation of precipitates in α-Al grain from the dissolved solutes in the aging (natural or artificial) step. Some initial heat treatment experiments were conducted on the samples cut from the tensile bars (~ 5 mm in thickness) to determine optimum heat treatment conditions which result without blister formation and allow most of the solute to be dissolved.

For the initial heat treatment experiments, three solutionizing temperatures were selected according to published literature namely 470, 490 and 510 ˚C [29–31]. Samples were heat-treated at these temperatures for 30, 60, and 120 min and quenched in room temperature water immediately in the end of heat treatments. After solution heat treatments microstructures of the samples were studied and hardness tests were conducted. Comparison of hardness values of as-cast and solution treated samples is shown in Fig. 1.

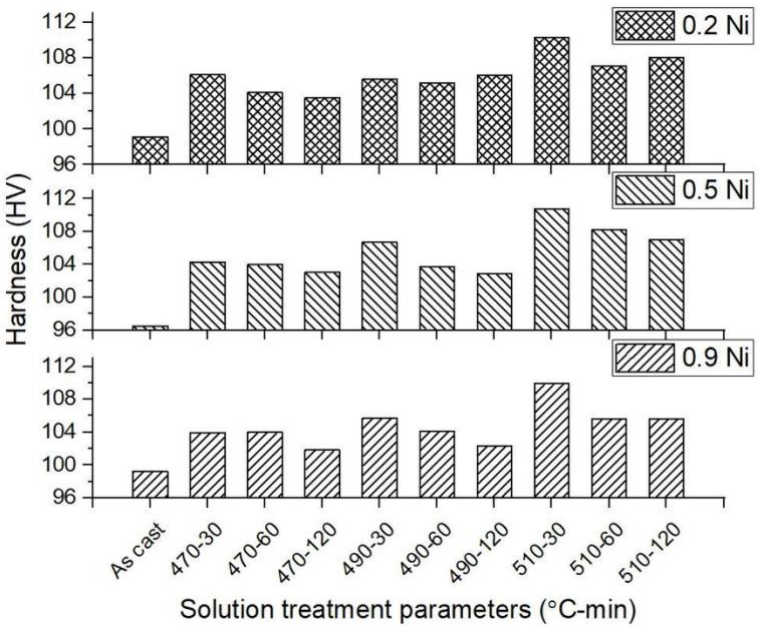

Fig. 1. A bar chart for hardness values of the three tested alloys after different solution treatment conditions. The standard deviation for each alloy is within ±1 HV.

Hardness results showed that maximum hardness was achieved at 30 min for all samples for selected temperatures; increased heat treatment durations caused a decrease in the hardness of the samples. An increment of hardness during solution heat treatment is expected as a result of increased solute atoms in the matrix due to the dissolution of the intermetallics. When intermetallics dissolve solute atoms increase hardness by solid solution hardening. Increased amount of solute content causes an increased hardness. But in the current study increased solutionizing times caused a drop in the hardness which may be a result of grain growth and Si coarsening. After analysing hardness data and microstructures of the materials optimum solution heat treatment duration was decided as 30 min because of the highest hardness values achieved. On the other hand, microstructural investigations showed that 30 min at 470 ˚C was not enough for the transformation of fibrous Si particles to a spherical morphology as can be seen in Fig. 2. As a result of this fact, further experiments at 470 ˚C were abandoned. Also, to understand whether it is possible to achieve similar hardness values with a shorter heat treatment an experiment was conducted at 510 ˚C for 20 min. Results of this extra experiment were promising (after solution treatment hardness of samples with 0.2, 0.5, and 0.9Ni was measured to be 118, 113, and 111 HV, respectively) so these samples were included in the aging treatments.

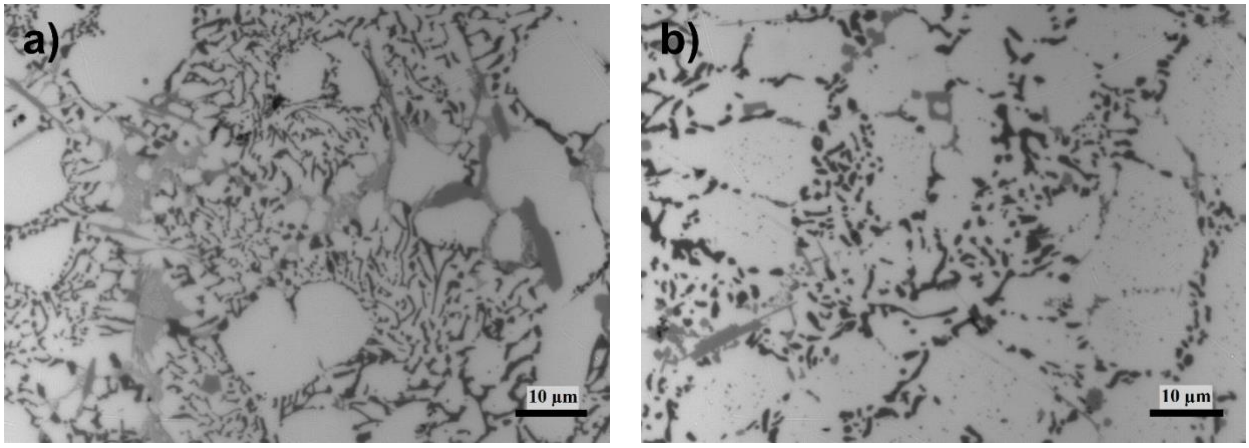

Fig. 2. Microstructure of 0.2Ni added sample, (a) as-cast and (b) after 470 ˚C – 30 min solution treatment

The aging temperature was kept constant at 190 ˚C for all samples. Samples were aged up to 14 hours and results of the hardness values are presented in Fig. 3. Hardness results of aged samples showed that maximum hardness is achieved after 30 min solution treatment at 510 ˚C followed by aging treatment for 6 hours at 190 ˚C. These parameters were used for the heat treatments of the tensile bars. Also, to see the effect of natural aging a set of tensile bars were solution treated at 510 ˚C for 30 min and then naturally aged at room temperature for 14 days.

An interesting result of the heat treatments was the low hardness of 0.2 and 0.9Ni containing alloys after heat treatments. In general, a higher amount of Ni is expected to cause an increase in the hardness as a result of higher volume fraction of intermetallics in the alloy. But, 0.9Ni added alloy exhibits the lowest hardness values for all heat treatment conditions, which is a result of the formation of Cu and Ni containing intermetallics. These intermetallics are stable at solution heat treatment temperatures as a result amount of dissolved solute is lower in this alloy. This phenomenon is discussed further in the next section.

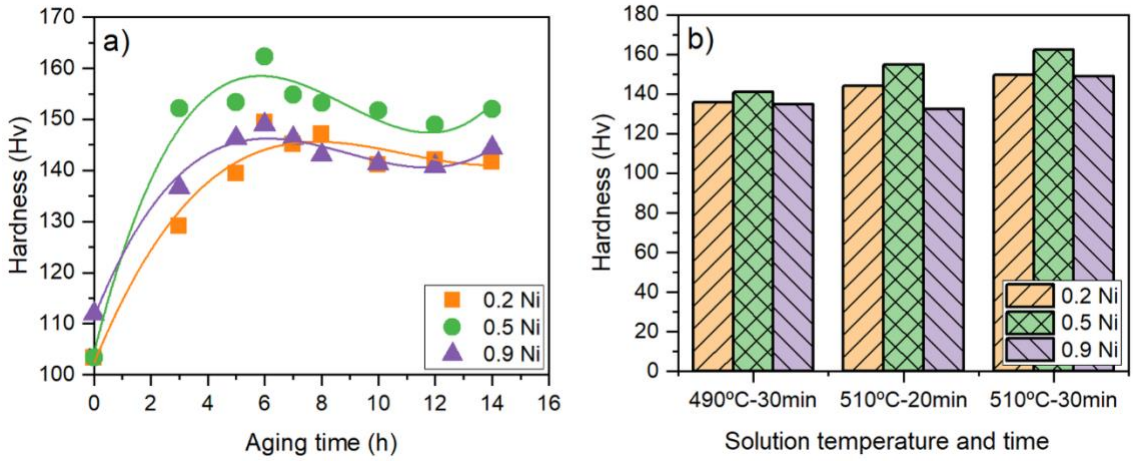

Fig. 3. (a) The aging curves at 190 ˚C for samples solution treated at 510 ˚C for 30 min. (b) The peak hardness values of all samples after different solution treated conditions, followed by aging at 190 ˚C

3.2. Microstructure

The as-cast state microstructure of A384 alloy consists of α-Al dendrites, eutectic Si particles, Al_2Cu intermetallics and some other Fe and/or Ni containing intermetallic phases. The amount of α-Al dendrites and eutectic phase depends on the Si content of the alloys. Higher amounts of Cu, Fe, and Ni in the alloy cause an increase in the amount of intermetallic phases. Because of the high cooling rates achieved with HPDC process some of the solute atoms are usually trapped inside α-Al grains which results with a smaller amount of intermetallics compared to the equilibrium conditions. For all of the alloys α-Al grains are the main constituent of the microstructure with the eutectic Si particles. The morphology of silicon particles is close to the fibrous type because of the modification effect of the added Sr. After solution heat treatment, Si particle morphology has transformed from fibrous to globular (Fig.4) and they are mainly located in the interdendritic borders.

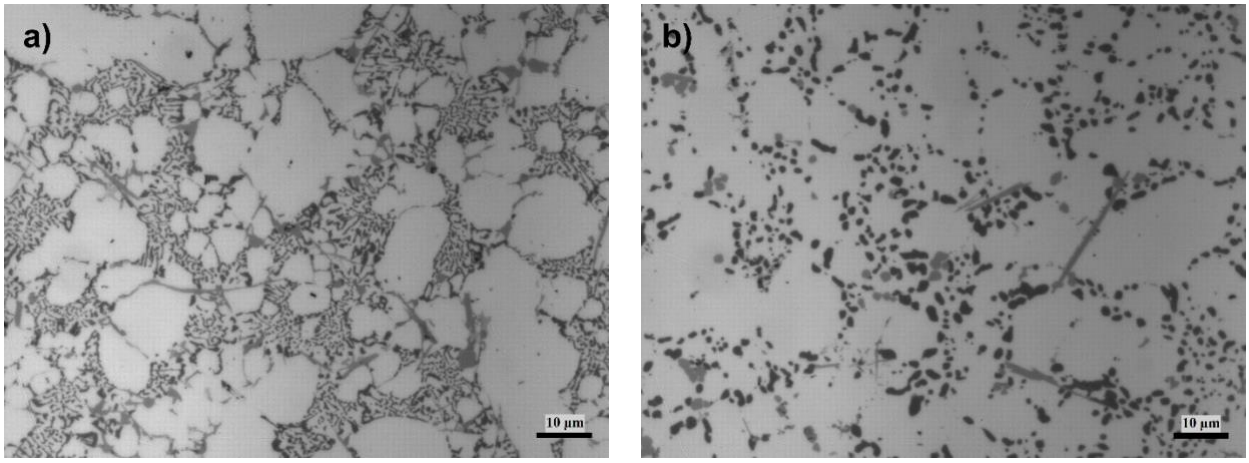

Fig. 4. Optical micrographs of 0.2Ni added sample before (a) and after (b) solution treatment (510 ˚C-30 min)

Another effect of solution heat treatment is dissolution of intermetallics at higher solutionizing temperature. As seen in the SEM images in Fig. 5 the amount of intermetallic phases decreases significantly when heat-treated at 510 ˚C for 30 min. However, it is clear from the images that the dissolution of intermetallics was not complete and some undissolved intermetallic crystals remain in the microstructure mainly located at the dendrite boundaries. It is also observed that amount of Ni in the alloys has an important effect on the chemical compositions of intermetallics that remain undissolved after solution heat treatments.

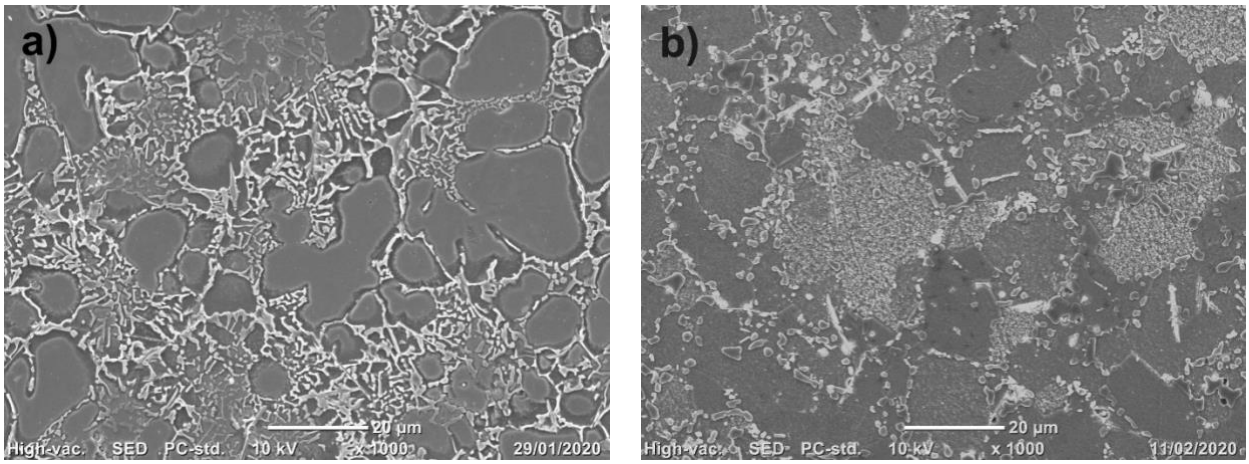

Fig. 5. SEM micrographs of 0.2Ni added sample before (a) and after (b) solution treatment (510 ˚C-30 min)

To understand the compositions of intermetallics, detailed EDS analyses were performed on numerous particles. The main intermetallic phases are Al_2Cu (θ), Al_5FeSi (β), $Al_{15}(Fe,Mn)_3Si_2$ (φ), Al_7Cu_4Ni (γ), Al_9FeNi (T), $Al_8FeMg_3Si_6$ (Q) and $Al_5Cu_2Mg_8Si_6$ (π). Although main reason of Mn addition is to prevent the formation of needle-shaped Al_5FeSi particles these particles are observed in the structure as a result of insufficient Mn addition.

Higher magnification SEM images of 0.2Ni added alloy before and after heat treatment are given in Fig. 6. Detailed EDS analyses proved that 0.2Ni added sample has Al_2Cu (θ), Al_5FeSi (β), Al_7Cu_4Ni (γ), $Al_{15}(FeMn)_3Si_2$ (φ), $Al_5Cu_2Mg_8Si_6$(π) and $Al_8FeMg_3Si_6$ (Q) phases. As can be seen from the microstructure of the heat-treated sample volume fraction of intermetallic phases decreases and the interconnected structure of intermetallics are no longer visible. The results of the image analysis on the as-cast and heat-treated samples showed that the area fraction of the intermetallics reduced from 6.01, 8.44 and 10.99 to 3.22, 5.91 and 6.58 % for 0.2, 0.5 and 0.9Ni containing alloys respectively.

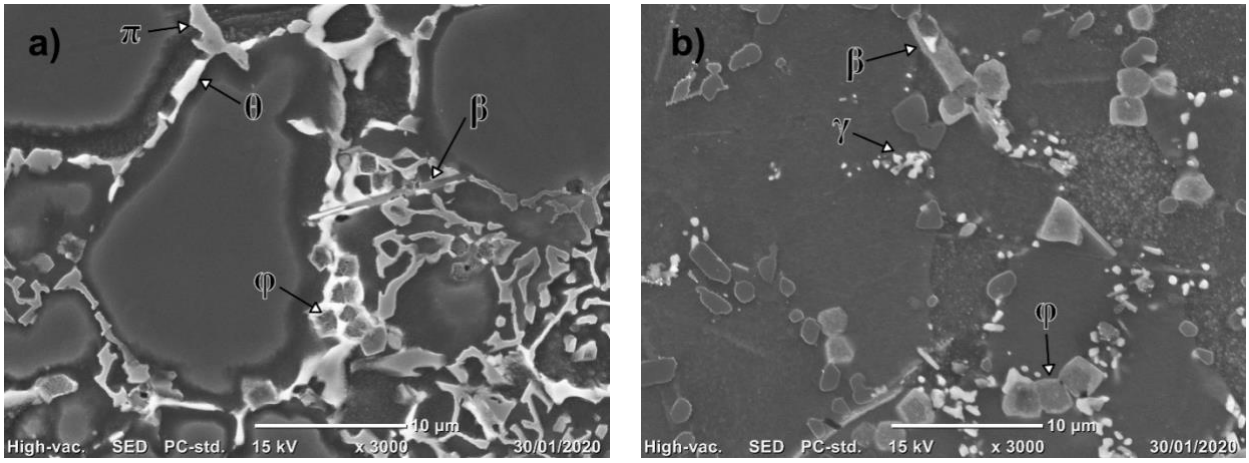

Fig. 6. SEM micrographs of 0.2Ni added sample (a) as cast and (b) solution treated (510 ˚C-30 min).

Similar intermetallics exist in the microstructure of 0.5 and 0.9Ni added samples. Representative SEM images before and after heat treatment for these alloys are given in Fig. 7 and Fig. 8 respectively. Defined possible phases in these samples are Al_3CuNi (δ), Al_7Cu_4Ni (γ), Al_9FeNi (T), $Al_{15}(FeMn)_3Si_2$ (φ), $Al_5Cu_2Mg_8Si_6$ (π), $Al_8FeMg_3Si_6$ (Q).

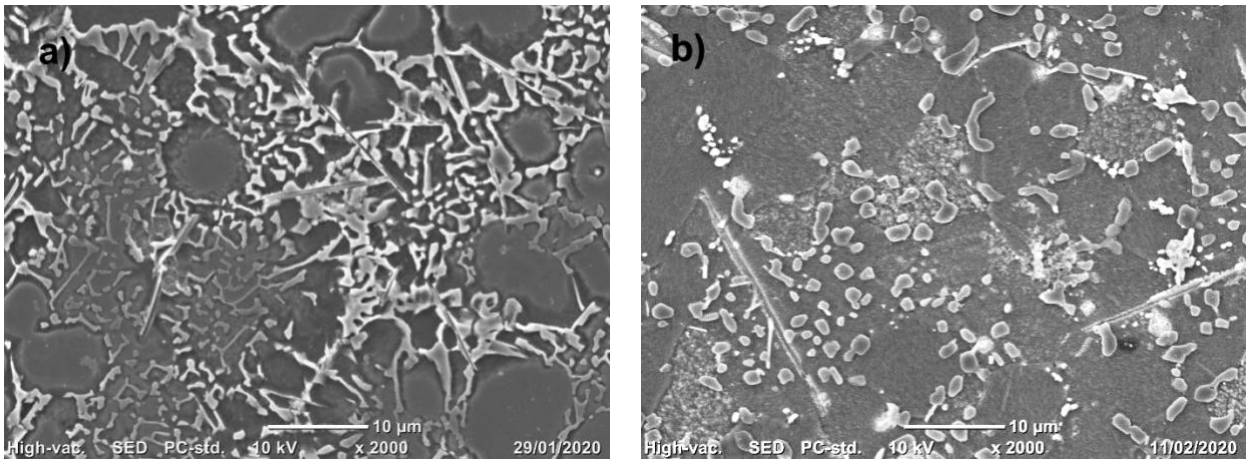

Fig. 7. SEM micrographs of 0.5Ni added sample (a) as-cast and (b) solution treated (510 ˚C-30 min)

When Ni content is increased to 0.5 some new intermetallics are observed to form whereas some of the intermetallics that were present in the 0.2Ni alloy disappeared. EDS analysis on 0.5Ni alloy reveals the absence of Al_5FeSi particles and increased amount of Al_7Cu_4Ni phase along with the formation of other Al_9FeNi and Al_3CuNi intermetallics.

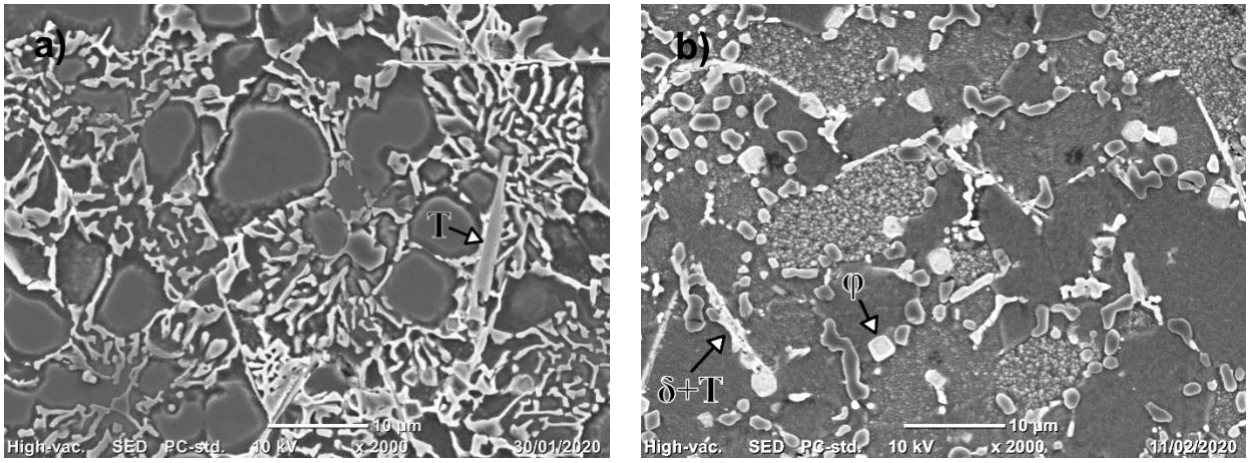

Fig. 8. SEM micrographs of 0.9Ni added sample (a) as-cast and (b) solution treated (510 ˚C-30 min)

Further increasing the Ni content to 0.9 increased the overall amount of $Al_3CuNi(\delta)$ phase significantly, however, the amount of $Al_7Cu_4Ni(\gamma)$ and $Al_9FeNi(T)$ phases are observed to be decreased. Microstructural features other than the intermetallic particles are not affected by the change in the Ni content of the alloys.

It is demonstrated [9] that the addition of Ni to Fe containing Al-Si-Cu alloys causes the formation of Al–Cu–Ni (Al_3CuNi or Al_7Cu_4Ni) and Al–Fe–Ni (Al_9FeNi) intermetallic phases. Results of the EDS analyses of the 0.5Ni added sample confirm the formation of the Al_9FeNi phase. In the alloy with 0.5Ni, Ni addition suppresses the formation of the Al_5FeSi phase since Fe tends to bond with Ni to form the Al_9FeNi phase [13, 25]. The negative effect of Al_5FeSi crystals on the ductility of Al-Si alloys is well known but the Al_9FeNi phase which forms instead of Al_5FeSi crystals is also detrimental to the ductility of the material because of its plate-like morphology. The plate-like morphology of Al_9FeNi can be seen in Fig. 8a and also reported in the literature [32].

The Al_9FeNi phase is not observed in the microstructure of 0.2Ni added sample and it has plate-like Al_5FeSi phase (Fig.6b) which causes a negative effect on the ductility. Other than that, the amount of the Al_2Cu (θ) phase was higher in the 0.2Ni added sample. When the Ni concentration is above 0.3, Al-Cu-Ni ternary intermetallics start to form [13]. For 0.5Ni containing alloy, the main ternary intermetallic is Al_7Cu_4Ni, whereas for 0.9Ni containing alloy the dominant phase is Al_3CuNi. The formation of these phases consumes Cu in the alloy and prevents the formation of Al_2Cu intermetallic. Also, the Al_2Cu phase can be easily dissolved with solution treatment but because of the stable nature of Ni-based intermetallics, their dissolution is limited [2]. The change in the chemical compositions of intermetallics directly affects the mechanical properties of the materials after heat treatment.

EDS analysis showed that the amount of Al_3CuNi phase with a short-strip or reticular morphology is higher in the 0.9Ni containing sample compared to the 0.5Ni added one. On the other hand, 0.5Ni added sample has more Al_7Cu_4Ni and Al_9FeNi phases than 0.9Ni added sample. Related studies and calculations show that with the increasing of Cu, Ni-phases transform from Al_3CuNi (δ) to Al_7Cu_4Ni (γ) phase and this transformation causes a great change in mechanical properties [14].

3.3. Tensile Properties

Tensile stress-strain curves of selected individual specimens and average values of all tensile tests results for as cast, naturally aged (510˚C-30 min, followed by 14 days aging at room temperature) and artificially aged (510˚C – 30 min, followed by 190˚C-6h) samples are given in Fig. 9 and Table 2 respectively. The results given in Table 2 are an average of at least three values.

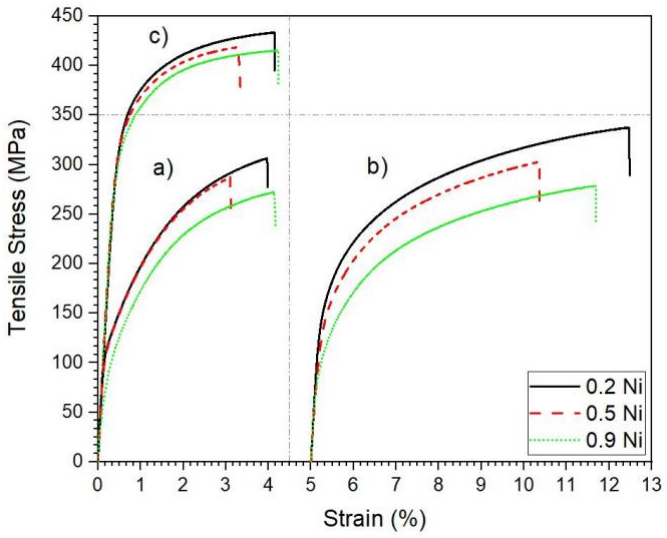

Fig. 9. Tensile properties of (a) as cast, (b) natural aged, and (c) artificially aged samples

It can be seen from the graphs that in the as-cast condition 0.9Ni containing alloy has lower strength compared to the other two alloys. The decrease in the strength of the alloys with increased Ni content can be attributed to increased volume fraction of the formed intermetallics. The EDS results showed that copper atoms and nickel atoms coexisted in the intermetallics. When the amount of the intermetallics increases this will lead to less dissolved copper in the matrix which causes a drop in the strength of the alloys. Whereas when the ductility of the alloys compared the highest and lowest Ni added alloys have similar values which are higher than the 0.5Ni added alloy. The trend in strength is the same after natural and artificial aging although the difference between 0.9Ni containing alloy and the others are smaller now. On the other hand, after two different aging

treatments, 0.9Ni containing alloy has higher elongation at break values than the 0.5Ni containing alloy, whereas 0.2Ni containing alloy has the highest elongation values.

Table 2. Average tensile test values of all samples

Type	Alloys	0.2 YS (MPa)	UTS (MPa)	Elongation (%)
As-Cast	0.2Ni	141.97 ± 7.42	301.6 ± 8.84	3.44 ± 0.62
	0.5Ni	146.23± 14.29	296.54± 13.78	2.88 ± 0.28
	0.9Ni	96.5 ± 4.71	255.63 ± 11.87	3.47 ± 0.47
Natural Aged	0.2Ni	163.83 ± 12.77	332.93 ± 9.61	6.75 ± 0.66
	0.5Ni	150.17 ± 3.91	298.1 ± 4.23	4.86 ± 0.35
	0.9Ni	120.9 ± 3.96	270.87 ± 6.65	6.52 ± 0.16
Artificial aged	0.2Ni	341.37 ± 6.48	429.93 ± 7.42	3.63 ± 0.62
	0.5Ni	336.53 ± 4.07	416.43 ± 2.12	2.72 ± 0.39
	0.9Ni	321.53 ± 2.74	408.1 ± 5.43	3.34 ± 0.59

4. Discussion

Detailed microstructural investigations conducted on as-cast and heat-treated alloys showed that the addition of different amounts of nickel to Al-Si-Cu alloys cast using HPDC method changes the chemical compositions of the intermetallics and their morphology significantly. Main intermetallic phases reported on the as-cast 0.2Ni containing alloy are Al_2Cu (θ), Al_5FeSi (β), $Al_{15}(Fe,Mn)_3Si_2$ (φ), Al_7Cu_4Ni (γ) and $Al_5Cu_2Mg_8Si_6$ (π) phases. Increasing Ni content to 0.5 suppresses the formation of Al_5FeSi phase and promotes the formation of Al_9FeNi phase and also some other phases like $Al_7Cu_4Ni$and Al_3CuNi. Further increasing the Ni content to 0.9 resulted with higher amounts of Al_3CuNi and lower amounts of Al_7Cu_4Ni and Al_9FeNi. The results of several EDS analyses on the microstructure of the as cast samples showed that no Al_3CuNi intermetallic was found in the 0.2Ni containing alloy whereas 6.25 and 13.16 % of the analysed intermetallic phases were Al_3CuNi in the 0.5 and 0.9Ni containing alloys respectively. The general trend of the intermetallics with increasing Ni in the alloy was decreasing the amount of Al_2Cu and Al_5FeSi and increasing Ni containing intermetallics. The change in the compositions and morphology of the intermetallics have a significant effect on the mechanical properties of the alloys.

Mechanical properties of HPDC Al-Si-Cu alloys are affected by many different parameters. Grain size and/or secondary dendrite arm spacing (SDAS) are one of the most prominent parameters. These microstructural parameters can be affected by different solidification rates and it is known that

alloying additions have an effect on grain size. In the current study, all samples were cast under the same conditions and no significant change in grain size was observed with the change of Ni in the alloy. Size and morphology of the secondary phases in the microstructure are the other important parameters that can significantly affect the mechanical properties of these alloys. The same amount of Sr was added to all alloys for modification of eutectic Si particles and microstructural investigations showed that for all alloys Si particles have similar size and morphology. Also, it is reported that the addition of Ni does not play a significant role on the morphology of Si particles [13, 25]. Small additions of Mn can improve the room and high-temperature tensile strength of these alloys [16]. In the current study, the effect of Mn on strength of the alloys was neglected as all samples have a similar amount of Mn. The addition of Mn causes formation of Al-Fe-Mn-Si phases, these phases usually have polyhedral or complex morphology. It is reported in the literature that Mn-rich phases have good thermal stability at 520°C [16]. Undissolved Mn containing phase (φ) after heat treatment can be seen in Fig. 6 and 8. Another minor alloying element in the studied alloys is magnesium. It is known that Mg plays an important role in rapid early hardening of Al-Si-Cu alloys [3]. Because all alloys in this study have similar levels of Mg the strength caused by this effect is same for all samples.

As shown in Table 2, in as-cast condition 0.2Ni and 0.5Ni containing alloys have similar strength but the ductility of 0.2Ni sample is higher than the 0.5Ni sample. The low ductility of 0.5Ni alloy compared to other alloys can be explained by the brittleness of Al_7Cu_4Ni phase. Figure 10 shows a SEM image taken on the fracture surface of a tensile sample and the EDS analysis of a brittle phase that has been fractured during the test. The result of the analysis shows that the brittle intermetallic consist of Al, Cu and Ni (Fe and Si in the analysis is a result of background) which suggests that this intermetallic is Al_7Cu_4Ni phase. The ease of the formation of crack on this intermetallic phase during the tensile test shows that this phase will act as a crack initiation point during the deformation and cause a decrease in the ductility of the material. Increasing nickel content from 0.2 to 0.5 increases the amount of Al_7Cu_4Ni phase which ends up with increased number of crack initiation points in the material resulting with low ductility compared to other alloys. On the other hand, although the addition of Ni causes a transformation from Al_5FeSi to Al_9FeNi, 0.5Ni is not enough for complete transformation and Al_9FeNi phase has also been reported as a brittle intermetallic [32]. This means some Al_9FeSi crystals are coexisting with Al_7Cu_4Ni crystals which have a negative effect on ductility. Increasing Ni content to 0.9 causes the formation of Al_3CuNi phase which results with a decrease in the amount of brittle Al_7Cu_4Ni and Al_9FeNi phases. On the other hand, Thermo-Calc modelling of the solidification of the alloys (not showed here) showed that solidification is

completed at a higher temperature for 0.9Ni containing alloy compared to the other alloys. When solidification is completed at a higher temperature this means more solute can be dissolved in the aluminium matrix which ends with less intermetallic formation. These differences in the amount and chemical composition of the intermetallics can be the reason of the low tensile strength and high ductility of the 0.9Ni containing alloy.

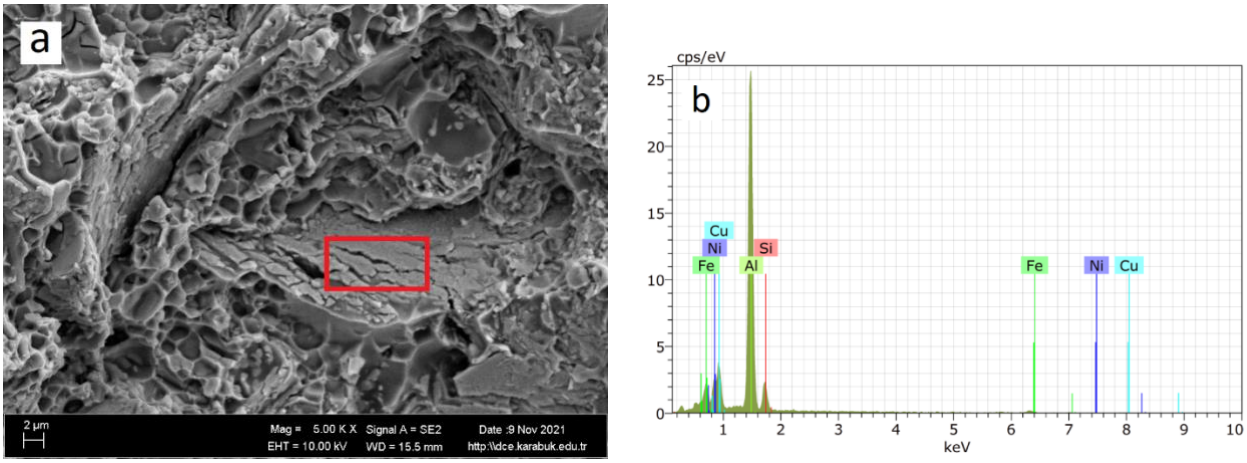

Fig. 10. (a) SEM image of 0.5 Ni alloy taken from fracture surface (b) EDS pattern of the cracked intermetallic marked with red rectangle

After natural aging treatment strength of all alloys have increased about 10 % but elongation values increased two-fold (Fig. 9). When artificially aged samples are compared with as-cast condition samples, elongation of the samples has similar values whereas UTS and YS increase about 50 % and over two-fold respectively (Fig. 9). The big difference in the elongation values of alloys after natural aging is a result of both spheroidization of Si crystals and the dissolution of some of the intermetallics. On the other hand, the small increase in the strength is a result of the formation of precipitates during natural aging, which can act as obstacles for dislocation movement. When artificial aging is applied to the specimens it is possible to form higher amount of precipitates in shorter times compared to natural aging because of increased temperature. The formation of higher amount of precipitates causes an increase in strength and a decrease in the elongation of all three alloys. The strength of the alloys after artificial aging decreases with increased Ni content. The reason for this is the formation of Ni containing intermetallics with Cu and Al. These intermetallic phases like Al_7Cu_4Ni and Al_3CuNi consume Cu in the alloy and decrease the amount of Al_2Cu. These Ni-containing phases are more stable at the solution heat treatment temperature and the tendency of them to get dissolved is low compared to the Al_2Cu phase. As a result, increasing Ni content results with fewer Cu atoms dissolved during solution heat treatment which leads to less precipitate formation during aging hence lower strength.

5. Conclusion

The results obtained during this study suggest that additions of Ni slightly below or above the standard limit (0.5 %), changes the intermetallic formation, which in turn affects the mechanical properties significantly. By increasing the Ni content, the fraction of Al_2Cu and Al_5FeSi decreases and also leads to formation of Ni containing intermetallics like Al_3CuNi, Al_7Cu_4Ni, and Al_9FeNi. The presence of different types of intermetallics and their volume fraction are observed to affect the mechanical properties. In as-cast condition, Ni addition (up to 0.5 %) is shown to increase the strength, whereas in the artificial aged condition, it decreases the strength. However, lower contents of Ni additions are desirable for improving the mechanical properties of A384 HPDC alloy under heat-treated conditions.

Acknowledgments

The first author was supported by The Scientific and Technological Research Council of Turkey (TUBITAK) under Grant 2219. The 2nd and 3rd authors acknowledge the financial support of the UK Engineering and Physical Science Research Council (EPSRC Grant: The Future Liquid Metal Engineering Research Hub, under grant number EP/N007638/1).

References

[1] Y.H Yoo, I.J. Park, J.G Kim, D.H Kwak, W.S. Ji, Corrosion characteristics of aluminum alloy in bio-ethanol blended gasoline fuel: Part 1. The corrosion properties of aluminum alloy in high temperature fuels, Fuel. 90 (2011) 1208–1214. https://doi.org/10.1016/j.fuel.2010.10.058

[2] H. Liao, G. Li, Q. Liu, Ni-Rich Phases in Al-12% Si-4% Cu-1.2% Mn-x% Ni Heat-Resistant Alloys and Effect of Ni-Alloying on Tensile Mechanical Properties, J. Mater. Eng. Perform. 28 (2019) 5398–5408. https://doi.org/10.1007/s11665-019-04307-5

[3] L. Wang, M. Makhlouf, D. Apelian, Aluminium die casting alloys: alloy composition, microstructure, and properties-performance relationships, Int. Mater. Rev. 40 (1995) 221–238. https://doi.org/10.1179/imr.1995.40.6.221

[4] L. Ceschini, I. Boromei, A. Morri, S. Seifeddine, I.L. Svensson, Microstructure, tensile and fatigue properties of the Al–10% Si–2% Cu alloy with different Fe and Mn content cast under controlled conditions, J. Mater. Process. Technol. 209 (2009) 5669–5679. https://doi.org/10.1016/j.jmatprotec.2009.05.030

[5] R. Baldan, J. Malavazi, A.A. Couto, Microstructure and mechanical behavior of Al9Si0. 8Fe alloy with different Mn contents, Mater. Sci. Technol. 33 (2017) 1192–1199. https://doi.org/10.1080/02670836.2016.1271966

[6] C.Y. Yang, S.L. Lee, C.K. Lee, J.C. Lin, Effects of Sr and Sb modifiers on the sliding wear behavior of A357 alloy under varying pressure and speed conditions, Wear. 261 (2006) 1348–1358. https://doi.org/10.1016/j.wear.2006.03.051

[7] T. Hosch, R.E. Napolitano, The effect of the flake to fiber transition in silicon morphology on the tensile properties of Al–Si eutectic alloys, Mater. Sci. Eng. A. 528 (2010) 226–232. https://doi.org/10.1016/j.msea.2010.09.008

[8] F.J. Tavitas-Medrano, J.E. Gruzleski, F.H. Samuel, S. Valtierra, H.W. Doty, Effect of Mg and Sr-modification on the mechanical properties of 319-type aluminum cast alloys subjected to artificial aging, Mater. Sci. Eng. A. 480 (2008) 356–364. https://doi.org/10.1016/j.msea.2007.09.002

[9] L. Fang, X. Zhang, H. Hu, X. Nie, J. Tjong, Microstructure and tensile properties of squeeze cast aluminium alloy A380 containing Ni and Sr addition, Adv. Mater. Process. Technol. 3 (2017) 90–100. https://doi.org/10.1080/2374068X.2016.1247341

[10] M. Zamani, S. Seifeddine, M. Aziziderouei, The role of Sr on microstructure formation and mechanical properties of Al-Si-Cu-Mg cast alloy, in: B.A. Sadler (Ed.), Light Metals 2013, Springer, 2016, pp. 297–302.

[11] Y.H. Cho, H.C. Lee, K.H. Oh, A.K. Dahle, Effect of strontium and phosphorus on eutectic Al-Si nucleation and formation of β-Al5FeSi in hypoeutectic Al-Si foundry alloys, Metall. Mater. Trans. A. 39 (2008) 2435–2448. https://doi.org/10.1007/s11661-008-9580-8

[12] G. Wang, X. Bian, W. Wang, J. Zhang, Influence of Cu and minor elements on solution treatment of Al–Si–Cu–Mg cast alloys, Mater. Lett. 57 (2003) 4083–4087. https://doi.org/10.1016/S0167-577X(03)00270-2

[13] A.R. Farkoosh, M. Javidani, M. Hoseini, D. Larouche, M. Pekguleryuz, Phase formation in as-solidified and heat-treated Al–Si–Cu–Mg–Ni alloys: Thermodynamic assessment and experimental investigation for alloy design, J. Alloys. Compd. 551 (2013) 596–606. https://doi.org/10.1016/j.jallcom.2012.10.182

[14] Y.Yang, K. Yu, Y. Li, D. Zhao, X. Liu, Evolution of nickel-rich phases in Al–Si–Cu–Ni–Mg piston alloys with different Cu additions, Mater. Des. 33 (2012) 220–225. https://doi.org/10.1016/j.matdes.2011.06.058

[15] X. Suo, H. Liao, Y. Hu, U.S. Dixit, P. Petrov, Formation of Al15Mn3Si2 phase during solidification of a novel Al-12% Si-4% Cu-1.2% Mn heat-resistant alloy and its thermal stability, J. Mater. Eng. Perform. 27 (2018) 2910–2920. https://doi.org/10.1007/s11665-018-3133-0

[16] F. Stadler, H. Antrekowitsch, W. Fragner, H. Kaufmann, P.J. Uggowitzer, Effect of main alloying elements on strength of Al–Si foundry alloys at elevated temperatures, Int. J. Cast. Met. Res. 25 (2012) 215–224. https://doi.org/10.1179/1743133612Y.0000000004

[17] A.M.A. Mohamed, F.H. Samuel, Microstructure, tensile properties and fracture behavior of high temperature Al–Si–Mg–Cu cast alloys, Mater. Sci. Eng. A. 577 (2013) 64–72. https://doi.org/10.1016/j.msea.2013.03.084

[18] J. Feng, B. Ye, L. Zuo, R. Qi, Q. Wang, H. Jiang, R.Huang, W. Ding, Effects of Ni content on low cycle fatigue and mechanical properties of Al-12Si-0.9 Cu-0.8 Mg-xNi at 350 C, Mater. Sci. Eng. A. 706 (2017) 27–37. https://doi.org/10.1016/j.msea.2017.08.114

[19] C.L Chen, A. Richter, R.C. Thomson, Mechanical properties of intermetallic phases in multi-component Al–Si alloys using nanoindentation, Intermetallics. 17 (2009) 634–641. https://doi.org/10.1016/j.intermet.2009.02.003

[20] N.A. Belov, D.G. Eskin, N.N. Avxentieva, Constituent phase diagrams of the Al–Cu–Fe–Mg–Ni–Si system and their application to the analysis of aluminium piston alloys, Acta. Mater. 53 (2005) 4709–4722. https://doi.org/10.1016/j.actamat.2005.07.003

[21] A.R. Farkoosh, M. Pekguleryuz, The effects of manganese on the T-phase and creep resistance in Al–Si–Cu–Mg–Ni alloys, Mater. Sci. Eng. A. 582 (2013) 248–256. https://doi.org/10.1016/j.msea.2013.06.030

[22] C.L. Chen, R.C. Thomson, The combined use of EBSD and EDX analyses for the identification of complex intermetallic phases in multicomponent Al–Si piston alloys, J. Alloys. Compd. 490 (2010) 293–300. https://doi.org/10.1016/j.jallcom.2009.09.181

[23] R.N. Lumley, R.G. O'Donnell, D.R. Gunasegaram, M. Givord, Heat treatment of high-pressure die castings, Metall. Mater. Trans. A. 38 (2007) 2564–2574. https://doi.org/10.1007/s11661-007-9285-4

[24] Committee ASMIH. ASM Handbook: Properties and Selection: Nonferrous Alloys and Special-Purpose Materials (ASM Handbook) VOL. 2. ASM International; 1990.

[25] C.B. Basak, A. Meduri, N.H. Babu, Influence of Ni in high Fe containing recyclable Al-Si cast alloys, Mater. Des. 182, 108017. https://doi.org/10.1016/j.matdes.2019.108017

[26] L. Fang, X. Zhang, L. Ren, H. Hu, X. Nie, J. Tjong, Effect of Ni addition on tensile properties of squeeze cast Al alloy A380, Adv. Mater. Process. Technol. 4 (2018) 200–209. https://doi.org/10.1080/2374068X.2017.1411746

[27] G.H. Garza-Elizondo, A.M. Samuel, S. Valtierra, F.H. Samuel, Effect of transition metals on the tensile properties of 354 alloy: role of precipitation hardening, Int. J. Met. 11 (2017) 413–427. https://doi.org/10.1007/s40962-016-0074-y

[28] X. Dong, H. Youssef, Y. Zhang, H. Yang, S. Wang, S. Ji, Advanced heat treated die-cast aluminium composites fabricated by TiB_2 nanoparticle implantation, Mater. Des. 186, 108372. https://doi.org/10.1016/j.matdes.2019.108372

[29] P. Krishnankutty, A. Kanjirathinkal, M.A. Joseph, M. Ravi, Effect of aging time on mechanical properties and wear characteristics of near eutectic Al–Si–Cu–Mg–Ni piston alloy, Trans. Indian. Inst. Met. 68 (2015) 25–30. https://doi.org/10.1007/s12666-015-0584-y

[30] R.N. Lumley, D.R. Gunasegaram, M. Gershenzon, R.G. O'Donnell, Effect of alloying elements on heat treatment response of aluminium high pressure die castings, Int. Heat. Treat. Surf. Eng. 4 (2010) 25–32. https://doi.org/10.1179/174951409X12542264514004

[31] H.M. Medrano-Prieto, C.G. Garay-Reyes, C.D. Gómez-Esparza, I. Estrada-Guel, J. Aguilar-Santillan, M.C. Maldonado-Orozco, R.Martinez-Sanchez, Effect of Nickel addition and solution treatment time on microstructure and hardness of Al-Si-Cu aged alloys, Mater. Charact. 120 (2016) 168–174. https://doi.org/10.1016/j.matchar.2016.08.020

[32] J. Rakhmonov, G. Timelli, F. Bonollo, Characterization of the solidification path and microstructure of secondary Al-7Si-3Cu-0.3 Mg alloy with Zr, V and Ni additions, Mater. Charact. 128 (2017) 100–108. https://doi.org/10.1016/j.matchar.2017.03.039